RSC Advances

PAPER

View Article Online
View Journal | View Issue

Cite this: *RSC Adv.*, 2018, **8**, 16910

Enhanced chondrogenic differentiation of human mesenchymal stems cells on citric acid-modified chitosan hydrogel for tracheal cartilage regeneration applications

Hao Chen,†[a] Hao Wang,†[a] Biyun Li,†[b] Bei Feng,[ac] Xiaomin He,[ac] Wei Fu,[ac] Huihua Yuan *[b] and Zhiwei Xu*[ac]

Congenital tracheal stenosis in infants and children is a worldwide clinical problem. Tissue engineering is a promising method for correcting long segmental tracheal defects. Nonetheless, the lack of desirable scaffolds always limits the development and applications of tissue engineering in clinical practice. In this study, a citric-acid-functionalized chitosan (CC) hydrogel was fabricated by a freeze–thaw method. Fourier transform infrared spectroscopy (FTIR) and X-ray diffraction (XRD) confirmed that citric acid was successfully attached to the chitosan hydrogel. Scanning electron microscopy (SEM) images and compression tests showed that the CC hydrogel had an interconnected porous structure and better wet mechanical properties. Using morphological and proliferation analyses, cell biocompatibility of the CC hydrogel was shown by culturing human mesenchymal stem cells (hMSCs) on it. Specific expression of cartilage-related markers was analyzed by real-time polymerase chain reaction and western blotting. The expression of chondrocytic markers was strongly upregulated in the culture on the CC hydrogel. Hematoxylin and eosin staining revealed that the cells had the characteristic shape of chondrocytes and clustered into the CC hydrogel. Both Alcian blue staining and a sulfated glycosaminoglycan (sGAG) assay indicated that the CC hydrogel promoted the expression of glycosaminoglycans (GAGs). In a nutshell, these results suggested that the CC hydrogel enhanced chondrogenic differentiation of hMSCs. Thus, the newly developed CC hydrogel may be a promising tissue-engineered scaffold for tracheal cartilage regeneration.

Received 26th January 2018
Accepted 30th April 2018

DOI: 10.1039/c8ra00808f

rsc.li/rsc-advances

1. Introduction

Congenital tracheal stenosis in infants and children, usually caused by local tracheal cartilage dysplasia, is one of the most challenging subjects in the field of tracheal medicine. Nowadays, the common treatment of tracheal stenosis is tracheal resection and end-to-end anastomosis. In contrast, if the tracheal defects are long circumferential (>50% of total tracheal length in adults and ~30% in children), clinicians may need to use tracheal graft reconstruction with suitable biofunctions.[1] The use of allografts, autografts, and synthetic materials is limited due to the lack of healthy donors, the risk of immune rejection, and poor biocompatibility, respectively.[2] Lately, the use of tissue-engineered tracheal grafts (a cellular or acellular graft) is a promising method for treatment of tracheal stenosis because of biological structures and functions similar to those of a native trachea.[3] In this regard, both synthetic and natural biomaterials have been employed with various results to select the most appropriate tracheal substitute. Compared with synthetic biomaterials, natural biomaterials are more acceptable because of their well-established biocompatibility and biofunctional properties.[4]

Chitosan (CTS), a natural cationic polysaccharide, is regarded as the most promising biomaterial for tissue-engineered scaffolds and tissue repair.[2] CTS has been shown to possess several excellent properties such as nontoxicity, stability, biodegradability, and biocompatibility, in addition to being inexpensive compared with other biomaterials.[5,6] Furthermore, CTS hydrogels have been used as cartilage tissue-engineered scaffolds because of their physical three-dimensional (3D) network and chemical structure similar to those of glycosaminoglycans (GAGs) of cartilage.[7,8] Nonetheless, a CTS hydrogel has limited mechanical strength, with compressive modulus in

[a]*Department of Pediatric Cardiothoracic Surgery, Shanghai Children's Medical Center Affiliated to Shanghai Jiao Tong University School of Medicine, Shanghai 200127, China. E-mail: xuzhiwei@scmc.com.cn*

[b]*School of Life Sciences, Nantong University, Nantong, Jiangsu 226019, China. E-mail: yuanhh@ntu.edu.cn*

[c]*Institute of Pediatric Translational Medicine, Shanghai Children's Medical Center, Shanghai Jiao Tong University School of Medicine, 1678 Dong Fang Road, Shanghai 200127, China*

† These authors contributed equally.

the range of 5.2–520 kPa.[9–13] Therefore, it is difficult to use a CTS hydrogel by itself for medical applications, especially as a tracheal cartilage scaffold material. To enhance mechanical properties of CTS-based scaffolds, extensive efforts have been made, such as altering the properties of a CTS solution (concentration, pH, or a solvent system),[14–16] addition of reinforcement agents or another synthetic or natural polymer, or chemical cross-linking treatment.[17–24] Nevertheless, most of these improved CTS scaffolds always have drawbacks, such as the presence of toxic chemicals[25] and/or limited controllability of structure and properties, which may be undesirable for an expected application.

Citric acid is a kind of ternary organic carboxylic acid that is part of in the Krebs cycle and is used in many fields, such as food, cleaning, and medical products.[26] Some studies on citric acid as a nontoxic cross-linker for CTS have also shown promising results for woolen fabrics,[27] *in situ* bone regeneration,[28] and healing of osteochondral defects.[29] A citric-acid-modified CTS film may promote biomineralization for bone tissue engineering.[30] Thus, citric acid plays a key role in these CTS-based biomaterials. On the other hand, these CTS-based biomaterials have not been used in tracheal tissue engineering. This study was aimed at producing a citric-acid-functionalized CTS (CC) hydrogel by the freeze-thawing technique, and we used citric acid as a bioactive molecule to enhance mechanical strength and biocompatibility of CTS for tracheal tissue engineering. After evaluating the mechanical properties of CC hydrogels and examining their biological properties, we concluded that CC hydrogels could be applied to induce human mesenchymal stems cells (hMSCs) to differentiate into chondrocytes for tracheal cartilage repair.

2. Experimental section

2.1 Materials

CTS (≥95% deacetylated) was acquired from Aladdin (Shanghai, China). Acetic acid, citric acid, and sodium hydroxide (NaOH) were all supplied by Sinopharm Chemicals (Shanghai, China). hMSCs (bone marrow, SCSP-405) were kindly provided by Stem Cell Bank, Chinese Academy of Sciences (Shanghai, China). All these chemicals were used as received without further purification.

2.2 Preparation of the CC hydrogels

First, CTS was dissolved in a 3% (w/v) acetic acid solution overnight to make CC solutions at the defined concentrations of 2 wt%. Then, 0.3 wt% citric acid was added to the solution. Next, 10 mL of each solution was poured into a template and frozen at −20 °C. After 12 h, the gels were thawed in 0.5 M NaOH solutions at room temperature to form CC hydrogels. After thawing, the CC hydrogels were immediately washed with deionized water until pH became neutral. As a control, a 2 wt% CTS hydrogel without modification was produced *via* a similar process.

2.3 Characterization of the CC hydrogels

Fourier transform infrared spectroscopy (FTIR) spectra of citric acid, CTS, and CC were obtained using a Tensor 27 FTIR spectrometer (Bruker, Germany) in the wavelength range of 500–4000 cm^{-1} at a scanning resolution of 4 cm^{-1}.

An X-ray diffractometer (D/Max-2550 PC, Rigaku, Japan) was used to determine the X-ray diffraction (XRD) pattern of citric acid, CTS, and CC with Cu Kα radiation in the $2\theta = 5$–60° range.

The morphology of the CC hydrogel samples was examined by scanning electron microscopy (SEM, TM-1000 Hitachi) at an accelerating voltage of 15 kV, and the pore size of the samples was measured by analysis of the SEM micrographs in five different areas in the ImageJ software. Porosity (ε) of the synthesized cryogels was determined according to the following equation: $\varepsilon = (1 - \rho/\rho_0) \times 100\%$, where ρ is the bulk polymer density, and ρ_0 is the density of the polymer scaffolds.

Compression tests were carried out on CTS and CC hydrogels. The height of cylindrical samples was 5 mm, and their diameter was 13 mm. All the samples were saturated with phosphate-buffered saline (PBS) and were employed for conducting compression tests. Uniaxial stress was applied directly to the cylindrical cryogel samples by means of a Materials Testing System AGS-500ND (Japan) with a 50 N load cell under displacement control at the rate of 1 mm min^{-1}. Cyclic compression was measured until axial strain reached 60% with 20 cycles. Recovery measurements were performed in PBS, and the constructs were allowed to recover for 1 min after every cycle.[31] Other parameters were consistent with the unconfined compression test parameters.

2.4 Flow-cytometric analysis

First, hMSCs were cultured in Dulbecco's Modified Eagle's Medium (DMEM) mixed with 10% of fetal bovine serum (FBS) and 1% of a streptomycin–penicillin antibiotic solution. Then, hMSCs were trypsinized and resuspended in icy PBS containing 0.1% of sodium azide and 1% of bovine serum albumin (Sigma-Aldrich). The cells (10^6) were incubated with antibodies specific to human cell surface antigens CD73, CD90, CD105, CD34, and CD45 (BD Biosciences) for 30 min at 4 °C. The samples were analyzed by flow cytometry (BD Biosciences, Franklin Lakes, NJ, USA).

2.5 Multipotent differentiation

As previously described, the multilineage differentiation potential of hMSCs in terms of osteogenesis, adipogenesis, and chondrogenesis was investigated.[32] Briefly, hMSCs were cultured at a density of 5×10^3 cells per cm^2 in low-glucose DMEM with 10% FBS, 10 mM β-glycerophosphate, 50 μg mL^{-1} L-ascorbic acid 2-phosphate, 0.1 μM dexamethasone (Sigma-Aldrich), and antibiotics for osteogenesis. The cells were fixed with 60% isopropanol and stained with Alizarin Red (Rowley Biochemistry, Danvers, MA, USA) for 21 days. hMSCs were induced to differentiate at a density of 10^4 cells per cm^2 in high-glucose DMEM with 10% FBS, 1 mM dexamethasone, 0.5 mM 3-isobutyl-1-methylxanthine, 1 mg mL^{-1} insulin

(Sigma-Aldrich), and antibiotics for adipogenesis. The cells were fixed with 4% formaldehyde and stained with Oil Red O (Sigma-Aldrich) for 21 days. hMSCs (2.5×10^5) were centrifuged at $600 \times g$ for 5 min and induced to differentiate in high-glucose DMEM with 1% ITSþ Premix (BD Biosciences), 0.9 mM sodium pyruvate (Sigma), 50 mg mL^{-1} L-ascorbic acid 2-phosphate, 10^{-7} M dexamethasone, 40 mg mL^{-1} L-proline (Fluka Analytical), and 10 ng mL^{-1} transforming growth factor beta 1 (TGF-B1; Peprotech Rocky Hill, NJ, USA) for chondrogenesis. The cell pellets were harvested on day 21, fixed with 4% formaldehyde, embedded in paraffin, and sectioned. The slices were deparaffinized, rehydrated, and stained with Alcian Blue (Polysciences).

2.6 Cell seeding

CC hydrogels (100 μL of a solution) were prepared in a 24-well plate. The resultant hydrogels were balanced with a cell culture medium. hMSCs resuspended in the medium were seeded onto the CC hydrogels in the presence of DMEM supplemented with 10% of FBS and 1% of the streptomycin–penicillin antibiotic solution (2.0×10^6 cells per well).

2.7 Cell morphology

Cell morphology was examined by SEM after 7 days of culture. Briefly, after the medium in 24-well plates was removed, and the cells were washed with PBS three times, the cell-scaffold constructs were fixed in 500 μL of 2.5% glutaraldehyde for 4 h at room temperature. After three washes with PBS, the constructs were further dehydrated in a graded series of alcohol solutions and dried overnight. Finally, the treated samples were sputter-coated with gold and platinum for SEM.

2.8 A cell proliferation assay

Cell proliferation was tested by a 3-(4,5-dimethylthiazol-2-yl)-2,5-diphenyltetrazolium bromide (MTT) assay at the predetermined culturing time points of 1, 4, and 7 days according to the manufacturer's instructions. Briefly, the cells were washed with PBS three times, and then 50 μL (5 mg mL^{-1}) of MTT was added into each well and incubated for 4 h. After that, 400 μL of DMSO (Sigma) was added into each well to dissolve the purple MTT formazan crystals for 15 min on a stirrer. Finally, the solutions were transferred to a 96-well plate to test optical density (OD) at 490 nm on a microplate reader (MK3, Thermo, USA).

2.9 The chondrogenic differentiation of MSCs on a CC hydrogel

To detect the chondrogenic differentiation of MSCs cultured on a CC hydrogel, the mRNA expression of hyaline cartilage-specific markers such as *SOX9*, type 2 collagen (*COL2*), and aggrecan (*AGN*) was examined by quantitative reverse-transcription polymerase chain reaction (qRT-PCR) after 7 days or 21 days of culture. Briefly, total RNA was first isolated using the TRIzol Reagent (Invitrogen, Carlsbad, CA). Then, first-strand cDNA was reverse-transcribed with the High Capacity cDNA Reverse Transcription Kit (Applied Biosystems, USA). Finally, RT-qPCR was performed using the SYBR Green Reagent Kit (Tiangen, Beijing, China) and an Applied Biosystems 7300 System (Applied Biosystems, USA). All primer sequences are listed in Table 1. The relative mRNA quantification of each gene was carried out by the $2^{-\Delta\Delta C_t}$ method, and data were normalized to control gene *GAPDH*.

The expression of chondrogenic markers, such as SOX-9, COL2, and AGN, was also detected by western blot analysis. hMSCs were lysed in RIPA buffer (Sigma-Aldrich, USA). Next, 20 μg of protein was loaded onto the 10% polyacrylamide gels (Bio-Rad, USA) for electrophoresis and then transferred to a polyvinylidene fluoride membrane (Bio-Rad, USA). Western blotting was performed with the following primary antibodies: an anti-SOX9 antibody (Abcam Cambridge, UK), anti-collagen Type II (Millipore Corp., USA), anti-aggrecan (Abcam, Cambridge, UK), and an anti-GAPDH antibody (Abcam), with a horseradish peroxidase-conjugated goat anti-mouse IgG antibody (Abcam) as the secondary antibody. The immuno-detected protein bands on the membrane were visualized using a ChemiDoc™ MP System (Bio-Rad, USA).

Twenty-one days later, cell-scaffold constructs were harvested for histological analysis. After that, the samples were fixed in 4% paraformaldehyde, dehydrated in an alcohol series, soaked with xylene, and embedded in paraffin. The samples were then cut into slices of 8 μm on a microtome. The slices were deparaffinized, rehydrated, and stained for hematoxylin & eosin (H&E) and Alcian Blue.

Cell-scaffold constructs after 21 day culture were digested in a papain (Sigma-Aldrich) solution at 60 °C for 20 h. Total sulfated glycosaminoglycan (sGAG) was then quantified through a reaction with 1,9-dimethylmethylene blue by means of the Blyscan Glycosaminoglycan Assay Kit (Biocolor, UK). The results were normalized to the total DNA amount, which was determined separately by the PicoGreen Assay (Invitrogen).

2.10 Statistical analysis

All the values were expressed as the mean ± standard error of at least three samples. Statistical analysis was performed by unpaired Student's t test. Data with $P < 0.05$ were considered statistically significant.

Table 1 Primer sequences for quantitative RT-PCR analysis[a]

Gene name	Accession number	Primer sequences (5′ to 3′)
GAPDH	NM_002046.3	F: CTCTCTGCTCCTCCTGTTCG
		R: TTAAAAGCAGCCCTGGTGAC
SOX9	NM_000346.3	F: TAAAGGCAACTCGTACCCAA
		R: ATTCTCCATCATCCTCCACG
COL2	NM_001844.4	F: CCTCTGCGACGACATAATCT
		R: CTCCTTTCTGTCCCTTTGGT
AGN	NM_013227.2	F: CACGATGCCTTTCACCACGAC
		R: TGCGGGTCAACAGTGCCTATC

[a] Forward and reverse primers are indicated as "F" and "R", respectively.

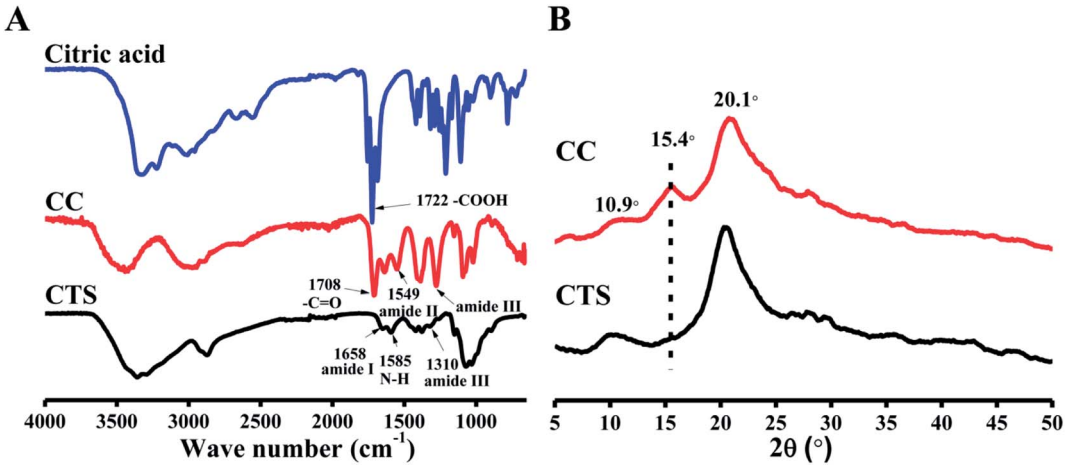

Fig. 1 FTIR spectra (A) and XRD (B) of citric acid, CTS and CC.

3. Results and discussion

3.1 FTIR spectroscopy and XRD analysis

Fig. 1A shows the FTIR spectra of citric acid, CTS, and CC. In the CTS FTIR spectrum, characteristic bands of CTS were observed at 1658 cm^{-1} (amide I) and 1585 cm^{-1} ($-NH_2$ bending),[33,34] but the amide III band at 1310 cm^{-1} was very weak. For CC, the peak intensities of –COOH in citric acid and unreacted amino groups at 1585 cm^{-1} both decreased. Meanwhile, a new peak at 1549 cm^{-1} (amide II) appeared, and an amide III band at ~1310 cm^{-1} increased, indicating formation of an amide bond. Moreover, the stretching vibration of C=O from the ester bond (at ~1730 cm^{-1}) was not found, which implied that –COOH in citric acid did not react with –OH in CTS, and it can be proposed that the fundamental reaction is mostly amidation: a reaction between the carboxyl in citric acid and the amino groups in CTS chains.[35]

The XRD method determines a material's crystal structure by measuring the position and intensity of its crystal diffraction peaks. XRD patterns of citric acid, CTS, and CC are illustrated in Fig. 1B. For CTS, this analysis clearly showed that a weak diffraction peak of 10.9°(020) and an intense diffraction peak of 20.1°(100) are caused by the crystallinity of CTS.[36] For CC, intensity of the peaks at 10.9° and 20.1° decreased due to the modification with citric acid. A new peak around 15.4° appeared in the curve of CC. This peak was caused by citric acid in CC.

Collectively, the FTIR and XRD results indicated that CTS was successfully modified with citric acid. The gelling mechanism implied that the partially unreacted carboxyl groups of CC reacted with NaOH and formed sodium citrate, which represents a multivalent anion and immediately induces ionic cross-linking of CC, thus forming a gel.[29,37]

3.2 Morphological analysis

For tissue engineering, a highly porous structure with interconnectivity that maintains good nutrient flow and metabolic exchange is necessary for a scaffold to ensure cell proliferation and growth. The preparation of CTS and CC hydrogels by the freezing–thawing method is a general technology for preparation of porous materials using ice formwork. The synthesized hydrogel had enough structural strength to support its weight, and a continuous porous gel skeleton could be observed in a cross-sectional SEM micrograph of the hydrogel. The CTS hydrogel clearly showed shriveled pore morphology (Fig. 2A) and lower porosity (80.5% ± 0.9%). In contrast, the CC hydrogels manifested pore morphology (Fig. 2B) and greater porosity (89.2% ± 1.3%). It is noteworthy that the pore wall of CC was

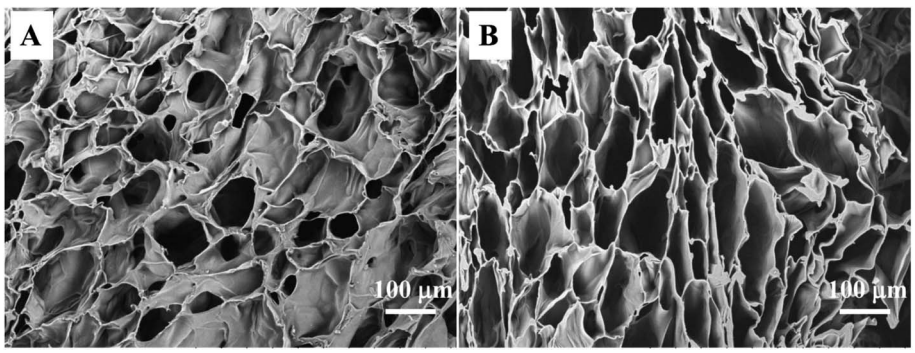

Fig. 2 SEM images of the CTS hydrogel (A) and CC hydrogel (B).

stronger than that of CTS, thus leading to higher mechanical strength as well as improved structural integrity. Although there were noticeable differences in pore morphology and porosity between CTS and CC hydrogels, all pore sizes were assumed to be appropriate for chondrocyte growth.[38] Therefore, the freezing–thawing method can be easily used for preparation of uniform porous scaffold materials for trachea tissue engineering applications.

3.3 Mechanical properties

Hydrogels for regeneration of tracheae should have sufficient mechanical strength at the site of application to maintain structural integrity. Unconfined compression tests were performed to generate experimental stress–strain data on the CTS and CC hydrogels, and assays were also performed to calculate their elastic modulus. CC hydrogels showed elastic behavior up to ~60% compression. Thereafter, the sharp increase in stress suggested that the stress was transferred from the hydrogels to the fixture. There was an interesting feature of CC hydrogels: they could be compressed up to 80% of their original length. The CTS hydrogels showed much worse compression mechanical properties (Fig. 3A). Elastic modulus of CC hydrogels measured at 30% compression (0.5 ± 0.17 MPa) is ~9-fold higher than that of CTS hydrogels (0.05 ± 0.02 MPa; Fig. 3B). Because of cross-linking with citric acid, CC hydrogels manifested mechanical characteristics closer to those of the human trachea (8.76 to 16.92 MPa).[39] The recovery of CTS and CC hydrogels after repetitive axial compression was also measured. CTC showed an obvious resistance decline and inability to restore the initial height (Fig. 3C). By contrast, CC hydrogels fully recovered after 20 cycles of repetitive 60% axial strain (Fig. 3D). The above results provide us with a comprehensive understanding of this new family of biodegradable elastic high-strength hydrogels. The CC hydrogels hold promise as scaffold materials for tracheal tissue engineering.

3.4 *In vitro* cell adhesion and proliferation assays

To show that CC hydrogels have the potential to serve as a scaffold for tracheal tissue, we initially chose hMSCs cultured on the CC hydrogels to test the material for cell adhesion and growth. First, the expression of cell surface antigens was analyzed by flow cytometry. The results revealed that the cells positive for mesenchymal makers CD73, CD90, and CD105 reached a proportion up to 99.9%, 99.8%, and 99.6%, respectively; whereas cells negative for a pan leukocyte marker (CD45) were scarce: 0.7% (Fig. 4A). Furthermore, we induced the cells to undergo osteo-, chondro-, and adipogenic differentiation to evaluate their multipotency. Alizarin red, Alcian blue, and Oil red O staining indicated that the cells were able to differentiate into osteo-, chondro-, and adipogenic lineages after 21 days of induction, respectively (Fig. 4B). Collectively, these characterization results suggested that we successfully isolated and maintained MSCs that were capable of multilineage differentiation. Fig. 5A and B revealed good adherence and growth of

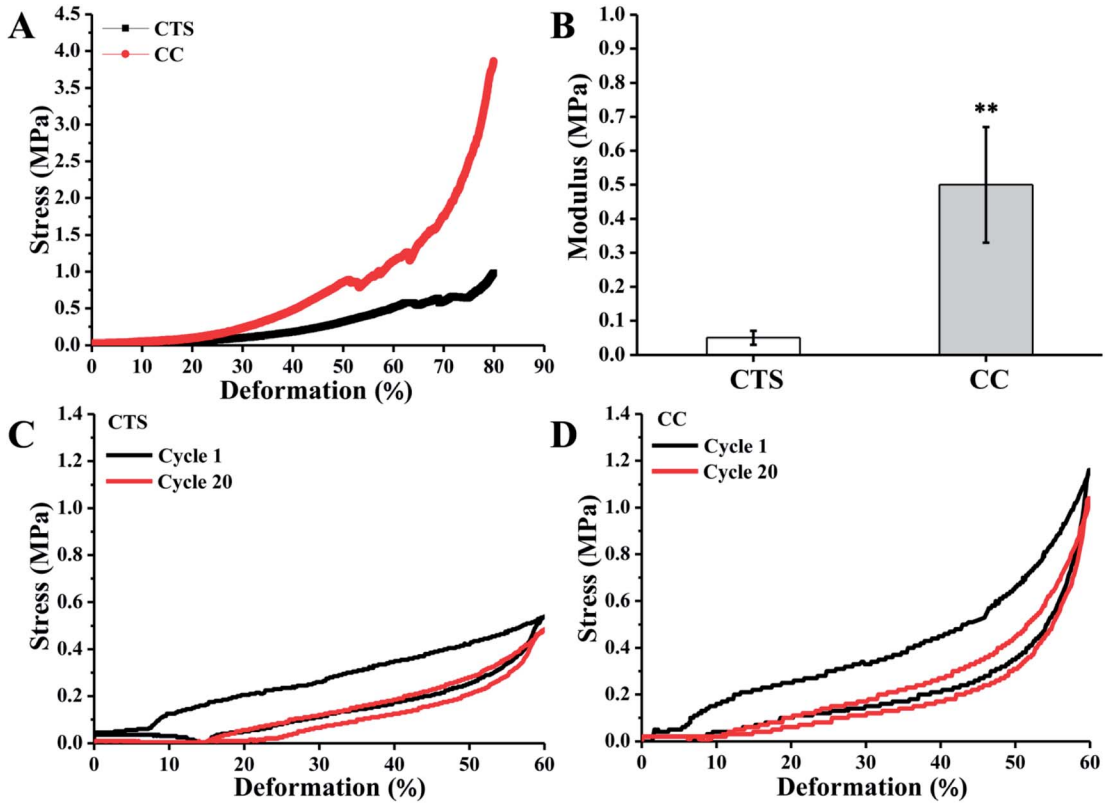

Fig. 3 Compressive stress–strain behavior of the CTS and CC hydrogels (A), the corresponding compression modulus at 30% deformation (B). The stress–strain curves of the first and last of 20 cycles of 60% compression are shown for (C) CTS hydrogel, (D) CC hydrogel. $^{**}p < 0.01$, $n = 5$.

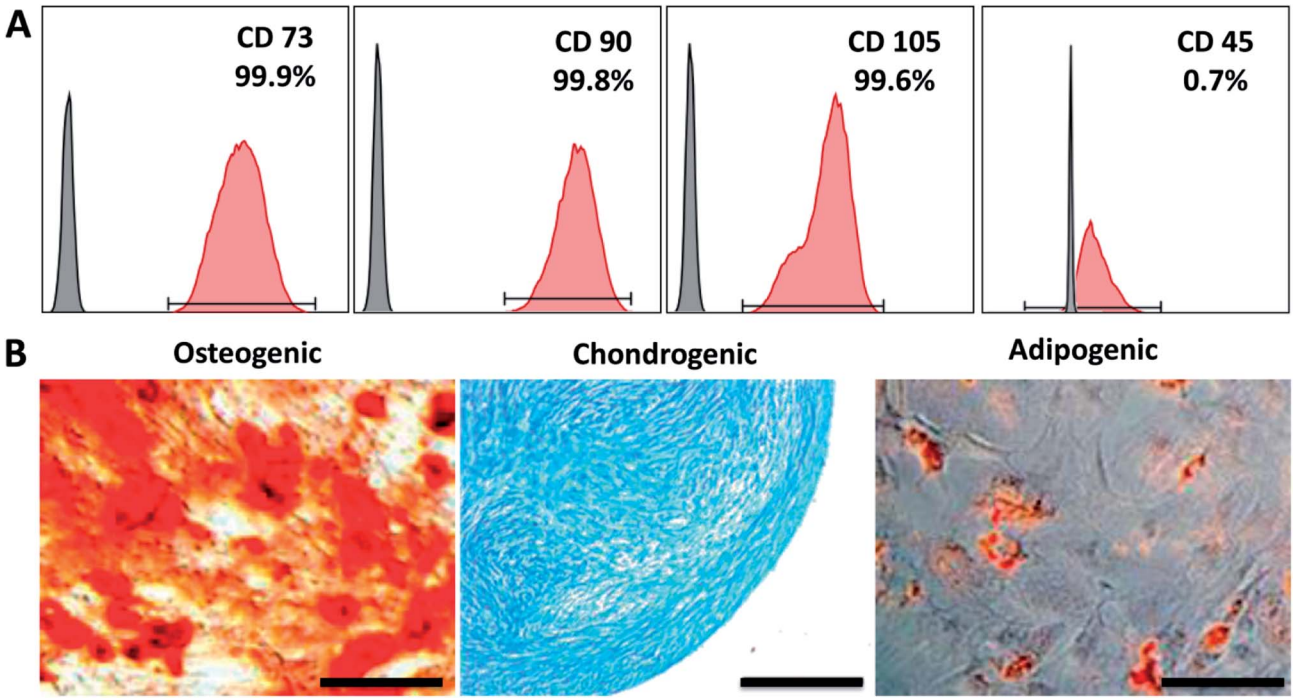

Fig. 4 Characterization of hMSCs surface antigens using flow cytometry (A) and multilineage differentiation (osteo-, chondro-, and adipogenesis) of hMSCs induced for 21 days were analyzed by the staining of Alizarin Red, Alcian Blue, and Oil Red O, respectively (B). Scale bar: 200 μm.

hMSCs on the CTS and CC hydrogel matrix. The CTS-based hydrogel scaffolds were able to provide an excellent microenvironment with interconnected pores for hMSCs to grow, especially the CC hydrogel, suggesting that the cells might have recognized the bioactive nature of CC and as a result adhered well; this finding revealed that the pores of the CC hydrogel appear to be large enough to allow cells to migrate into the pores of the hydrogel matrix and to enable effective mass transport and nutrient supply, which are essential for effective cell growth.[40,41] Moreover, cells on the CC hydrogel showed the characteristic shape of chondrocytes. Thus, the above results all indicate that the CC hydrogel provides a native like environment for chondrocyte growth.

The growth and proliferation of hMSCs in CC hydrogels was also examined at predetermined time points by the MTT assay. The biocompatibility of the CC hydrogels was compared with that of the CTS hydrogel. Moreover, the CC hydrogels manifested the capacity for increasing cellular metabolic activity of hMSCs as time goes on, as shown in Fig. 5C. An increase in the cell metabolic activity as measured by the MTT assay indicates good cell adhesion and proliferation in the CC hydrogels. The cell growth rate in the CC hydrogels suggested their good potential for lengthy tracheal healing applications to enable generation of the new tissue.

3.5 The chondrogenic differentiation of MSCs cultured on scaffolds

To investigate the ability of the CC hydrogel to promote hMSC chondrogenesis, hMSCs were cultured on the CTS hydrogel as a control. Several studies have indicated that CTS-based scaffolds are effective at preserving the phenotype of chondrocytes and their ability to synthesize collagen II and GAG.[42,43] To quantify the mRNA expression of cartilage-related markers, we conducted qRT-PCR to analyze the hMSCs in CTS or CC

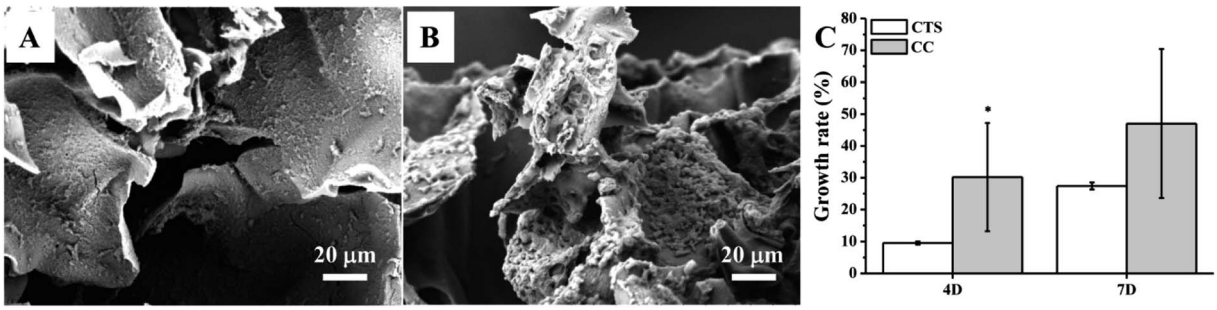

Fig. 5 SEM images of hMSCs cells grown in CTS (A) and CC (B) hydrogel at 7 days of the culture. (C) Proliferation of hMSCs on the CC hydrogel. (*$p < 0.5$, $n = 3$).

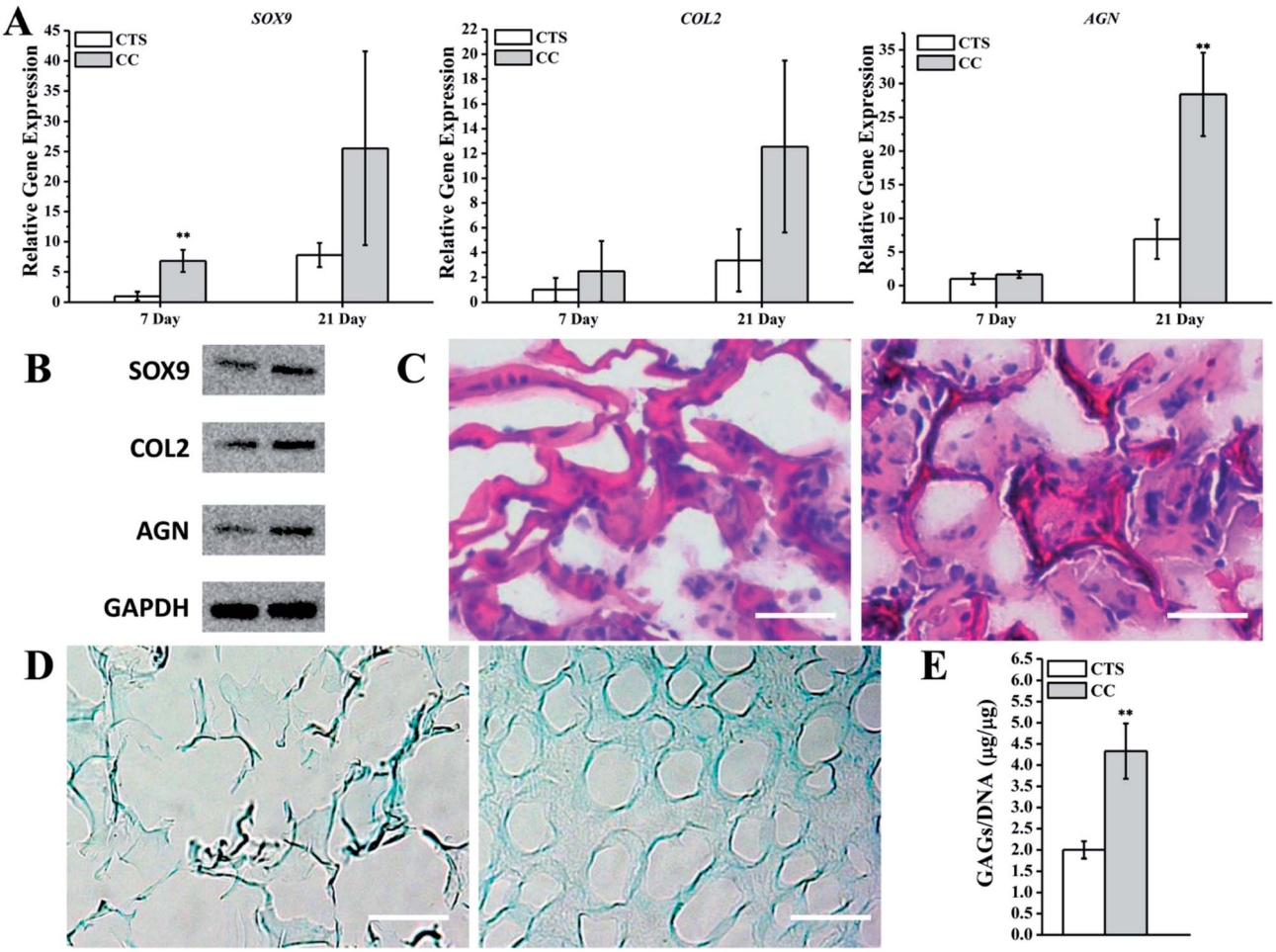

Fig. 6 Analysis of the chondrogenic capacity of hMSCs cultured on CTS and CC hydrogel. (A) mRNA transcript levels of cartilage-related markers of hMSCs were analyzed using quantitative RT-PCR. (B) Western Blot analysis of chondrogenesis proteins after hMSCs was cultured for 21 days. (C and D) Histologic analysis of hMSCs cultured on CTS and CC hydrogel for 21 days. Specimen sections were stained with (C) H & E or (D) Alcian Blue. Scale bar: 50 μm. (E) GAG production in hMSCs cultured with CTS or CC hydrogels was quantified and normalized with the total DNA amount. $^{**}p < 0.01$, $n = 3$.

hydrogels. The results revealed that the expression levels of *SOX9*, *COL2*, and *AGN* were all upregulated on CC hydrogels as compared with the CTS hydrogel on day 7. On day 21, expression levels in the culture with the CTS hydrogel were remarkably lower in comparison with CC hydrogels (Fig. 6A). The expression of these cartilage-specific proteins was also higher in CC hydrogels than in CTS hydrogels after 21 days (Fig. 6B). The analysis of H&E staining showed that cells on day 21 (hMSCs cultured on CC hydrogels) primarily resided in the region close to the pore wall of the hydrogels and produced the extracellular matrix in the spaces within the pores, whereas few cells were observed in CTS hydrogels (Fig. 6C). Alcian Blue staining showed that more GAGs were synthesized by hMSCs on CC hydrogels than on CTS hydrogels (Fig. 6D). Quantification of sGAG production revealed that the cells produced a greater amount of sGAG per cell on CC hydrogels than on the CTS hydrogel (Fig. 6E). These results suggested that CC hydrogels promoted hyaline chondrogenesis among hMSCs.

As we all know, the goal of tracheal engineering is cartilage regeneration. Thus, CC hydrogels are a suitable candidate for tracheal cartilage repair owing to their excellent physiochemical and biological properties. These hydrogels may provide excellent porosity for hMSC attachment and facilitate hMSC proliferation and chondrogenic differentiation.

4. Conclusions

A citric-acid-modified CTS (CC) hydrogel prepared by freeze-thawing was developed and has an elastic nature and high mechanical strength. The CC hydrogels also have a macroporous, interconnected pore morphology that allows for unhindered flow of nutrients and mass transport through the scaffold. In addition, biocompatibility and the cell–biomaterial interactions of the scaffolds were confirmed by means of hMSCs, which manifested good cell adhesion, proliferation, and secretion of the extracellular matrix in the CC hydrogel matrices. Moreover, the CC hydrogels enhanced chondrogenic differentiation of hMSCs *in vitro*. From these results, it is concluded that CC hydrogels have potential applications to tracheal cartilage regeneration.

Conflicts of interest

There are no conflicts to declare.

Acknowledgements

This work was supported by the National Natural Science Foundation of China (81370117), Six Talent Peaks Project in Jiangsu Province (XCL-063), the Nature Science Foundation of the Jiangsu Higher Education Institutions of China (16KJB540002), and Nantong applied research program (GY12016031). It is also funded by High Level Introduction of Talent Research Start-up Foundation of Nantong University (03081136, 03081135) and Large Instruments Open Foundation of Nantong University (KFJN1823).

Notes and references

1 H. C. Grillo, *Ann. Thorac. Surg.*, 2002, **73**, 1995–2004.
2 U. Abdulcemal Isik, E. Seren, I. Kaklikkaya, D. Bektas, M. Imamoglu, H. Muhtar and S. Civelek, *J. Thorac. Cardiovasc. Surg.*, 2002, **43**, 281–286.
3 R. Langer and J. P. Vacanti, *Science*, 1993, **260**, 920–926.
4 C. Chung and J. A. Burdick, *Adv. Drug Delivery Rev.*, 2008, **60**, 243–262.
5 E. Khor and L. Y. Lim, *Biomaterials*, 2003, **24**, 2339–2349.
6 M. Ignatova, N. Manolova, N. Markova and I. Rashkov, *Macromol. Biosci.*, 2009, **9**, 102–111.
7 M. Dash, F. Chiellini, R. M. Ottenbrite and E. Chiellini, *Prog. Polym. Sci.*, 2011, **36**, 981–1014.
8 A. Montembault, K. Tahiri, C. Korwin-Zmijowska, X. Chevalier, M. T. Corvol and A. Domard, *Biochimie*, 2006, **88**, 551–564.
9 P. B. Celine, V. Antoine, B. Denis, V. Laurent, D. Laurent and F. Catherine, *J. Appl. Polym. Sci.*, 2013, **128**, 2945–2953.
10 C. Yang, L. Xu, Y. Zhou, X. Zhang, X. Huang, M. Wang, Y. Han, M. Zhai, S. Wei and J. Li, *Carbohydr. Polym.*, 2010, **82**, 1297–1305.
11 Z. Ying, W. Lu, X. Ling, Z. Maolin and W. Shicheng, *Radiat. Phys. Chem.*, 2012, **81**, 553–560.
12 Y. Xu, D. Xia, J. Han, S. Yuan, H. Lin and C. Zhao, *Carbohydr. Polym.*, 2017, **177**, 210–216.
13 A. Subramanian and H. Y. Lin, *J. Biomed. Mater. Res., Part A*, 2005, **75**, 742–753.
14 S. Jana, S. J. Florczyk, M. Leung and M. Q. Zhang, *J. Mater. Chem.*, 2012, **22**, 6291–6299.
15 N. Bhattarai, J. Gunn and M. Zhang, *Adv. Drug Delivery Rev.*, 2010, **62**, 83–99.
16 Y. Sun, Y. Li, J. Nie, Z. Wang and Q. Hu, *Chem. Lett.*, 2013, **42**, 838–840.
17 T. Y. Chiang, C. C. Ho, D. C. H. Chen, M. H. Lai and S. J. Ding, *Mater. Chem. Phys.*, 2010, **120**, 282–288.
18 E. A. Elizalde-Pena, N. Flores-Ramirez, G. Luna-Barcenas, S. R. Vasquez-Garcia, G. Arambula-Villa, B. Garcia-Gaitan, J. G. Rutiaga-Quinones and J. Gonzalez-Hernandez, *Eur. Polym. J.*, 2007, **43**, 3963–3969.
19 L. Y. Jiang, Y. B. Li, X. J. Wang, L. Zhang, J. Q. Wen and M. Gong, *Carbohydr. Polym.*, 2008, **74**, 680–684.
20 T. Jiang, W. I. Abdel-Fattah and C. T. Laurencin, *Biomaterials*, 2006, **27**, 4894–4903.
21 Z. S. Li, H. R. Ramay, K. D. Hauch, D. M. Xiao and M. Q. Zhang, *Biomaterials*, 2005, **26**, 3919–3928.
22 A. M. Martins, C. M. Alves, F. K. Kasper, A. G. Mikos and R. L. Reis, *J. Mater. Chem.*, 2010, **20**, 1638–1645.
23 Z. S. Shen, X. Cui, R. X. Hou, Q. Li, H. X. Deng and J. Fu, *RSC Adv.*, 2015, **5**, 55640–55647.
24 H. C. Yu, H. Zhang, K. Ren, Z. Ying, F. Zhu, J. Qian, J. Ji, Z. L. Wu and Q. Zheng, *ACS Appl. Mater. Interfaces*, 2018, **10**, 9002–9009.
25 M. Z. Albanna, T. H. Bou-Akl, O. Blowytsky, H. L. Walters III and H. W. T. Matthew, *J. Mech. Behav. Biomed. Mater.*, 2013, **20**, 217–226.
26 D. Gyawali, P. Nair, Y. Zhang, R. T. Tran, C. Zhang, M. Samchukov, M. Makarov, H. K. W. Kim and J. A. Yang, *Biomaterials*, 2010, **31**, 9092–9105.
27 S. M. Gawish, S. M. A. El-Ola, A. M. Ramadan and A. A. Abou El-Kheir, *J. Appl. Polym. Sci.*, 2012, **123**, 3345–3353.
28 A. Sanchez-Ferrero, A. Mata, M. A. Mateos-Timoneda, J. C. Rodriguez-Cabello, M. Alonso, J. Planell and E. Engel, *Biomaterials*, 2015, **68**, 42–53.
29 P. Ghosh, A. P. Rameshbabu and S. Dhara, *Langmuir*, 2014, **30**, 8442–8451.
30 Y. Liu, X. Shen, H. Zhou, Y. Wang and L. Deng, *Appl. Surf. Sci.*, 2016, **370**, 270–278.
31 J. Visser, F. P. W. Melchels, J. E. Jeon, E. M. van Bussel, L. S. Kimpton, H. M. Byrne, W. J. A. Dhert, P. D. Dalton, D. W. Hutmacher and J. Malda, *Nat. Commun.*, 2015, **6**, 6933.
32 T. L. Tsai, B. C. Nelson, P. A. Anderson, T. A. Zdeblick and W. J. Li, *Spine J.*, 2014, **14**, 2127–2140.
33 N. Bhattarai, H. R. Ramay, J. Gunn, F. A. Matsen and M. Q. Zhang, *J. Controlled Release*, 2005, **103**, 609–624.
34 X. Qu, A. Wirsen and A. C. Albertsson, *J. Appl. Polym. Sci.*, 1999, **74**, 3193–3202.
35 M. Cai, J. Gong, J. Cao, Y. Chen and X. Luo, *J. Appl. Polym. Sci.*, 2013, **128**, 3308–3314.
36 B. Li, Y. Zhang, Y. Yang, W. Qiu, X. Wang, B. Liu, Y. Wang and G. Sun, *Carbohydr. Polym.*, 2016, **152**, 825–831.
37 X. Shu, K. Zhu and W. Song, *Int. J. Pharm.*, 2001, **212**, 19–28.
38 S. H. Oh, I. K. Park, J. M. Kim and J. H. Lee, *Biomaterials*, 2007, **28**, 1664–1671.
39 F. Safshekan, M. Tafazzoli-Shadpour, M. Abdouss and M. B. Shadmehr, *Materials*, 2016, **9**, 456.
40 N. Kathuria, A. Tripathi, K. K. Kar and A. Kumar, *Acta Biomater.*, 2009, **5**, 406–418.
41 P. Sarazin, X. Roy and B. D. Favis, *Biomaterials*, 2004, **25**, 5965–5978.
42 S. Yamane, N. Iwasaki, T. Majima, T. Funakoshi, T. Masuko, K. Harada, A. Minami, K. Monde and S. Nishimura, *Biomaterials*, 2005, **26**, 611–619.
43 D. L. Nettles, S. H. Elder and J. A. Gilbert, *Tissue Eng.*, 2002, **8**, 1009–1016.